New Phytologist

Research

Tree stem methane emissions are regulated by site-level biogeochemistry over species identity in Amazon floodplain forests

Holly R. Blincow[1], Niall P. McNamara[2], Dafydd M. O. Elias[2], Carla Gomez[1,3], Jack Lamb[4], Rodrigo Nunes de Sousa[1], Darlene Gris[5], Leonardo Pequeno Reis[5,6], Alison M. Hoyt[4] and Sunitha Rao Pangala[1,3]

[1]Lancaster Environment Centre, Lancaster University, Bailrigg, Lancaster, LA1 4YQ, UK; [2]UK Centre for Ecology & Hydrology, Lancaster, LA1 4AP, UK; [3]Department of Life Sciences, Imperial College London, Silwood Park Campus, Ascot, SL5 7PY, UK; [4]Department of Earth System Science, Stanford University, Stanford, CA, 94305-4216, USA; [5]Mamirauá Institute for Sustainable Development, Amazonas, 69470-000, Brazil; [6]Universidade Federal Rural da Amazônia, Belém, Pará, 66077-901, Brazil

Authors for correspondence:
Holly R. Blincow
Email: holly.blincow@cumbria.ac.uk

Sunitha Rao Pangala
Email: s.pangala@imperial.ac.uk

Received: *26 November 2025*
Accepted: *21 March 2026*

New Phytologist (2026)
doi: 10.1111/nph.71168

Key words: Amazon, CH_4, igapó, tree stem methane, tropical floodplain forests, várzea, wetlands.

Summary

- Tree stems in Amazonian floodplains emit substantial methane (CH_4), yet controls on emission variability remain unclear. Emissions span orders of magnitude between várzea (nutrient-rich) and igapó (nutrient-poor) forests and among trees, suggesting controls beyond flooding.
- We tested whether site-level biogeochemistry better explains stem CH_4 variability than species identity by measuring emissions from two co-occurring species with contrasting wood densities – *Eschweilera coriacea* and *Hevea spruceana* – across várzea and igapó forests. Emissions were paired with porewater chemistry (electrical conductivity, dissolved oxygen, dissolved CH_4, and dissolved organic carbon), methane production potential (MPP), and root biomass.
- Stem CH_4 emissions were significantly higher in várzea than in igapó, independent of species or stem height. Várzea porewaters displayed higher conductivity, dissolved CH_4 and MPP, near-neutral pH, and lower oxygen, with fine roots concentrated in the 0- to 50-cm soil layer, indicating a shallow CH_4 supply zone. Basal stem emissions in várzea correlated with shallow porewater chemistry and fine-root biomass, whereas relationships in igapó were weak.
- These findings show that Amazonian floodplain stem CH_4 emissions are governed by shallow site-level biogeochemistry, rather than species identity alone and should be incorporated into basin-scale CH_4 budgets and process models to capture spatial variability.

Introduction

Tropical wetlands are the largest natural source of atmospheric methane (CH_4), with the Amazon basin contributing a substantial proportion due to widespread annual flooding, which transforms over 800 000 km^2 into forested wetlands (Hess *et al.*, 2015; Saunois *et al.*, 2025). While CH_4 emissions have previously been attributed mainly to anoxic soils and waterbodies, recent studies have identified tree stems as major emission pathways, with emissions in Amazonian floodplain forests exceeding those of tropical peatlands and temperate wetlands by up to two orders of magnitude (Pangala *et al.*, 2013, 2017). Despite their global significance, the controls on CH_4 emissions from Amazonian tree stems remain poorly understood.

Two basin-scale studies show strong hydrological control on seasonal patterns (Pangala *et al.*, 2017; Gauci *et al.*, 2022), yet stem emissions vary by orders of magnitude among ecosystems and among trees within sites at single time points, implying additional controls beyond flooding (Pangala *et al.*, 2017; Gauci *et al.*, 2022). Proposed explanations point to interactions between woody traits (e.g. wood density, porosity, and lenticel abundance) and belowground biogeochemistry that shape CH_4 production, availability, transport, and subsequent emission (Pangala *et al.*, 2015; van Haren *et al.*, 2021; Soosaar *et al.*, 2022; Epron *et al.*, 2023; Moisan *et al.*, 2024). In the Amazonian floodplains, where within-season temperature is relatively stable, hydrology typically dominates seasonality (Pitz *et al.*, 2018; Gauci *et al.*, 2022); however, once flooded, increasing water depth does not necessarily increase emissions (Gauci *et al.*, 2022; Jeffrey *et al.*, 2023), suggesting that flooding serves as an 'on/off' switch for soil-driven methanogenesis, with finer-scale variability controlled by other variables.

Woody traits such as wood density, porosity, and anatomical adaptations have previously been linked to variability in stem CH_4 emissions. Lower density wood is often associated with higher emissions due to reduced diffusion resistance (Pangala *et al.*, 2014;

van Haren *et al.*, 2021; Soosaar *et al.*, 2022), while porosity, parenchyma, lenticel density, and moisture content also influence CH_4 emissions (Pangala *et al.*, 2015; Epron *et al.*, 2023). Tree functional traits shaped by flood adaptation may also interact with internal CH_4 production or oxidation processes within woody tissues (Parolin *et al.*, 2004; Epron *et al.*, 2023; Jeffrey *et al.*, 2023; Moisan *et al.*, 2024), making stem emissions potentially sensitive to species-specific anatomical characteristics. Because many of these traits covary among species (Chave *et al.*, 2009; Poorter *et al.*, 2010; Yang *et al.*, 2024), comparing species with contrasting wood density provides a practical way to test whether species identity helps explain variation in stem CH_4 emissions when the full suite of woody traits is not measured directly. However, in Amazonian floodplain forests, it remains unclear whether variation in stem CH_4 emissions is better explained by species identity, as a proxy for differences in wood structure and transport potential, or by site-level belowground biogeochemistry that governs CH_4 production and availability.

Amazonian flooded forests, with their unique water chemistry, present a particularly complex setting. White-water várzea floodplains receive Andean-derived, sediment-rich waters (electrical conductivity (EC) 50–150 μS cm^{-1}, near-neutral pH) while black-water igapó forests receive acidic (pH < 5), low-EC (< 50 μS cm^{-1}), nutrient-poor waters from weathered Guiana and Brazilian shields (Furch & Wolfgang, 1997; Junk *et al.*, 2011) – contrasts that shape microbial communities and methanogenic activity. These biogeochemical differences likely modulate soil CH_4 production and dissolved CH_4 availability for stem transport, driving spatial variability across the basin. Furthermore, porewater properties such as pH, dissolved oxygen (DO), electrical conductivity (EC), dissolved organic carbon (DOC), and dissolved CH_4 are also known to play significant roles in regulating soil methanogenesis and CH_4 availability (Wang *et al.*, 1996; Teh *et al.*, 2005; Liu *et al.*, 2012), while fine-root biomass density regulates local CH_4 production and availability through substrate supply and access to soil CH_4 (Aulakh *et al.*, 2001; Liu *et al.*, 2012; Bridgham *et al.*, 2013; Ge *et al.*, 2024; Määttä & Malhotra, 2024).

Although flooding is a prerequisite for anaerobic processes, the rate and magnitude of CH_4 production and emissions including stem emissions are expected to be shaped by these finer-scale belowground variables. Yet, stem CH_4 measurements have not been systematically paired with tree-specific porewater chemistry, methane production potential (MPP), and root biomass across this biogeochemistry gradient. Here, we address this gap by quantifying CH_4 emissions from two co-occurring species with contrasting wood density – *Eschweilera coriacea* (high wood density) and *Hevea spruceana* (low wood density) – in nutrient-rich white-water várzea and nutrient-poor black-water igapó during the flooded season. Using species identity as a proxy for contrasting wood density, we paired stem emission measurements with tree-specific porewater chemistry (pH, EC, DO, DOC, dissolved CH_4), MPP, and root biomass to 150 cm depth. We tested whether below-ground biogeochemistry better explains variability in stem CH_4 emissions than species identity across contrasting black- and white-water flooded forests.

Materials and Methods

Study site

The study was conducted in the central Amazonian floodplain of Brazil (*c.* 500 km west of Manaus) within two sustainable development reserves (Fig. 1): (i) a black-water igapó forest plot in Amanã Sustainable Development Reserve (ASDR; 2°38.598′S, 64°39.980′W; south of Amanã lake) and (ii) a white-water várzea forest plot in Mamirauá Sustainable Development Reserve (MSDR; 2°48.916′S, 65°05.192′W; near Japurá river). The igapó plot is influenced by two hydrologically distinct river systems: the white-water Solimões-Japurá confluence and the black-water Negro River. In the dry season, waters from the Solimões-Japurá dominate at the site, whereas in the flooded season, Negro River waters predominate. At the time of sampling, the site was inundated with *c.* 1.5 m of water. The igapó forest plot contains *c.* 500 trees within the 1 ha plot from 80 species (data provided by the Mamirauá Institute). The várzea forest plot was bounded by the Solimões, Japurá, and Auati Paraná Rivers and located close to the Japurá River along a smaller river channel. The várzea forest plot contains *c.* 400 trees within the 1-ha plot from 100 species (data provided by the Mamirauá Institute), with flooding of *c.* 4 m at the time of sampling. Understory vegetation is denser in igapó forests than in várzea, whereas aboveground biomass production is substantially higher in várzea reaching 17.4 t ha^{-1} compared with 8.7 t h^{-1} in igapó forests (Furch, 1997).

The two sites were chosen based on their contrasting hydrology: a nutrient-poor, low-pH, relatively high-DO black-water igapó with 1–2 m flooding for up to 45 d (igapó plot; Supporting Information Fig. S1), vs a nutrient-rich, sediment-laden white-water várzea with 2–4 m flooding for up to 3 months (várzea plot; Fig. S1). The mean annual temperatures at both plots were 27°C.

Within our 1-ha plots, two tree species, *Hevea spruceana* (Spruce ex Benth.) Müll.Arg. (Euphorbiaceae), commonly known as Seringa Barriguda, and *Eschweilera coriacea* (DC.) S.A.Mori (Lecythidaceae), commonly known as Matamata, were selected for this study. Five mature individuals of each species were sampled per plot. These species were chosen because they were among the few species occurring in both plots and represented contrasting wood densities, making them ideal for testing species identity as a proxy for woody traits. Across the two plots, only 10 species were shared, and *H. spruceana* and *E. coriacea* were the only pair with markedly different wood density (0.5 ± 0.2 g cm^{-3} for *H. spruceana* and 0.8 ± 0.08 g cm^{-3} for *E. coriacea*) (Table S1). Both species were sufficiently abundant (≥ 10 mature individuals per plot) and spatially distributed across each plot (trees ≥ 3–6 m apart), ensuring representative sampling without clustering bias. Both species are large canopy trees that occur in Amazonian forests but differ in habitat specialisation and wood structure. *Hevea spruceana*, a relative of the rubber tree *H. brasiliensis*, is primarily associated with seasonally flooded riverine environments and is characteristic of várzea and igapó forests, where it is adapted to periodic inundation (Wittmann *et al.*, 2006, 2010). By contrast, *E. coriacea* is one of the most widespread and abundant canopy tree species in

Fig. 1 Locations of the two field study plots in the Brazilian Amazon: the igapó site, situated within the Amanã Sustainable Development Reserve (in blue), and the várzea site, located within the Mamirauá Sustainable Development Reserve (in red).

Amazonia and occurs across a broader range of habitats, including both terra firme and seasonally flooded forests (Wittmann *et al.*, 2006; Steege *et al.*, 2013; Heuertz *et al.*, 2020). The two species therefore represent contrasting ecological strategies and wood densities, with *E. coriacea* typically forming dense hardwood characteristic of Lecythidaceae taxa, whereas *H. spruceana* exhibits lower wood density typical of many Euphorbiaceae species (Wycherley, 1992). Tree diameter at breast height ranged from 18 to 52 cm for *H. spruceana* and 19–50 cm for *E. coriacea* (Table S1).

Tree stem CH_4 measurements

Tree stem CH_4 emissions were measured during daylight hours over 3 wk in May 2022 in the flooded season at both plots (Table 1). Emissions were measured at two heights: 30–60 cm and 70–100 cm above the floodwater line (*c.* 1.5 m in igapó and *c.* 4 m in várzea), using chambers as described in Pangala *et al.* (2017). The flexible transparent polycarbonate chambers with neoprene gas tight foams around the edges were strapped to the stems using ratchet straps, and the visible gaps

Table 1 Summary of measurements by year and site for each field campaign.

Year	Site ID	Analysis
2019	Igapó; várzea	EC, pH, DO, fine-root biomass and coarse root biomass from three soil depths (0–50 cm, 50–100 cm, and 100–150 cm) per tree in each plot
2021	Igapó; várzea	EC, pH, DO, dissolved CH_4, DOC, MPP from three soil depths (0–50 cm, 50–100 cm, and 100–150 cm) per tree in each plot
2022	Igapó; várzea	Stem CH_4 emissions at two stem heights (30–60 cm and 70–100 cm) from five trees per species (*Eschweilera coriacea* and *Hevea spruceana*) per plot

around the edges were plugged with modelling clay. Once attached to the tree stems, the chambers were connected via gas-tight tubing to the microportable greenhouse gas analyser (ABB LGR GLA131-GGA), which analysed CH_4 concentration changes from the tree stem chamber in real time. CH_4 emissions were calculated based on the linear change in CH_4 concentration over time within the chamber headspace.

$$F = \frac{\mathrm{d}(CH_4)}{\mathrm{d}t} \times \frac{PV}{ART}$$

where F is the flux in mg m^{-2} h^{-1}, P is atmospheric pressure, T is temperature, R is the universal gas constant, A is the surface area of the chamber, and V is the volume of air enclosed by the chamber. A linear regression was applied to each 5-min chamber closure time series, and only emission estimates with a correlation coefficient (R^2) > 0.97 were retained for analysis (all emissions met this threshold). Final emission values are reported mg CH_4 m^{-2} h^{-1}, normalised to the stem surface area enclosed by the chamber.

Belowground measurements

Because of logistical constraints and pandemic-related travel disruptions, belowground measurements and stem emission measurements were not all measured in the same year; details of when each of the measurements were made are included in Table 1. Interannual comparisons (2019 vs 2021) of porewater chemistry (EC, pH and DO) indicated minimal variation between sampling campaigns.

Porewater chemistry

Porewater was sampled from standpipe piezometers constructed from PVC pipes, installed at depths of 0–50 cm, 50–100 cm, and 100–150 cm. Each piezometer had 3-mm holes drilled *c.* 1.5 cm apart within its designated 50-cm segment (0–50 cm, 50–100 cm, or 100–150 cm), with end caps fitted to the top of the piezometer to exclude rainwater. Water was extracted from the target depth via tubing connected to a peristaltic pump. During the dry season, piezometers were installed at the desired depths within a 50 cm radius around each monitored tree (20 trees in total; three piezometers per tree) and allowed to stabilise for a year before sampling commenced in May 2019 (Table 1). Each tree had its own set of piezometers at all three depths, enabling assessment of tree-specific effects relative to belowground conditions. No samples were collected during the 2022 campaign as piezometers were submerged under water.

Water samples extracted from piezometers were analysed for dissolved CH_4, DOC, pH, EC, and DO. Dissolved CH_4 concentrations were measured from the equilibrated headspace of porewater samples. 60 ml of porewater and 40 ml of atmospheric air were shaken vigorously for 5 min inside a 100-ml syringe, after which a 10-ml aliquot of atmospheric air was added to a 3-ml Exetainer vial (Labco, Lampeter, UK) for analysis of CH_4 concentrations using gas chromatography (GC) (Clarus 480 Perkin Elmer, Shelton, CT, USA). Samples were corrected for atmospheric contamination, and dissolved CH_4 concentrations were calculated from the headspace CH_4 mixing ratio using Henry's law, accounting for partitioning between water and gas phases and corrected for temperature at the time of equilibration using the NEONDISSGAS package (Cawley *et al.*, 2020).

Samples for DOC concentration were collected from piezometers at all depths and filtered through a Whatman 40-μm filter. Due to the remote location of sampling, all samples were placed on ice to keep them < 4°C while in the field. Samples were frozen within 14 d of collection for preservation (Cook *et al.*, 2016) and analysed using a Shimadzu TOC-L CPH analyser (Kyoto, Japan).

EC and pH were measured using a multiparameter pocket tester (Apera Instruments PC60 Premium, Shanghai, China). The handheld device was calibrated against a Hanna Instruments HI 2003 Edge® EC Meter and Hanna Instruments HI5221 pH Meter (Smithfield, RI, USA). EC reflects the concentration of dissolved ions in the water column and was used here as an indicator of differences in ionic and nutrient content between white-water (várzea) and black-water (igapó) floodplain environments, rather than as a measure of salinity. DO was analysed in porewater using a Hanna Dissolved Oxygen Meter (Model HI9143). Belowground samples were collected in the wet seasons of May 2019 and 2021. In May 2019, only DO, EC, and pH were measured, with analysis expanded in 2021 to include DOC and dissolved CH_4 (Table 1).

CH_4 production potential (MPP)

Intact soil cores were extracted to 150 cm during the wet season in 2021 using a Russian-type peat auger (Eijkelkamp, Giesbeek, the Netherlands) and sectioned into depth intervals of 0–5, 5–30, 30–50, 50–100, and 100–150 cm. Each section was placed into a gas-tight incubation container, consisting of a PVC pipe cut to fit the intact core and sealed with two PVC end caps. One end cap sealed the bottom of the core, and the other was attached to the top and fitted with a three-way valve for gas sampling. It was flushed with N_2 to establish anoxia and incubated in the dark at field temperature (average of 26°C) for 14 d. Headspace gas samples (2 ml) were withdrawn at 0, 6, 12, 24, 48, and 72 h, then every 24 h to Day 7 and every 48 h until Day 14, and analysed for CH_4 on a Shimadzu GC-FID (Kyoto, Japan), and replaced with equal volumes of N_2 to maintain pressure. MPP was calculated as follows:

$$\mathrm{MPP} = \frac{\Delta n CH_4}{A \Delta t}$$

where $\Delta n CH_4$ is the cumulative increase in moles of CH_4 in the headspace over the incubation interval (after correcting concentrations for N_2 backfilling), and $A\Delta t$ is the product of the core cross-sectional area and incubation time, giving units of mmol CH_4 m^{-2} h^{-1}, which were converted to mg CH_4 m^{-2} h^{-1} using the molar mass of CH_4.

Root biomass

Three soil cores per tree per depth were extracted using a soil auger (5 cm diameter, 150 cm long) in May 2019 (wet season). The soil cores were extracted within a 75 cm radius around the tree (same 20 trees that were measured for tree stem emissions), with samples taken at three soil depths, with three replicates at each depth: 0–50 cm, 50–100 cm, and 100–150 cm. Root biomass was measured by separating roots from the soil by wet sieving and manual sorting, and separating roots >2 mm (coarse roots) and <2 mm (fine roots) in diameter. Roots were then oven-dried at 60°C for 72 h and weighed to determine root biomass per volume of soil.

Although roots from neighbouring trees may also have been present within the sampled volume, focal trees were generally well-spaced (most separated from their nearest neighbours by *c.* 3 m in igapó and *c.* 5 m in várzea), so sampling within a 75 cm radius of each stem likely captured a substantial proportion of roots from the focal tree and its immediate neighbourhood while not guaranteeing exclusive attribution.

Root biomass measurements preceded stem CH_4 emission measurements by *c.* 2 yr (2019 vs 2022). Although absolute root biomass may vary between years due to turnover, the vertical distribution of roots in mature Amazon floodplain forests is largely structured by the annual flood pulse, which regulates oxygen availability and root development (Parolin *et al.*, 2004; Wittmann *et al.*, 2010). Root dynamics typically vary more across hydrological phases within a year than between years within the same season. As both root sampling and emission measurements were conducted during the flooded season, they represent comparable stages of the flood cycle. We therefore interpret the observed root distribution as representative of the relative rooting environment influencing methane supply, recognising that interannual turnover may affect absolute biomass but is unlikely to change the vertical pattern or its relationship with stem CH_4 emissions.

Statistical analysis

All statistical analyses were conducted in R v.12.0. Normality was visually assessed, and data were transformed where necessary. Stem CH_4 emissions were analysed with linear models (log-transformed), including site, species, height, and two-way interactions. Model simplification was guided by Akaike's Information Criterion (AIC), with residuals inspected for assumption violations.

The effect of belowground parameters (EC, DO, pH, MPP) on dissolved CH_4 was analysed with linear mixed effect models including tree species, site, soil depth, and tree identity as a random effect. We also tested for species-dependent effects by including an interaction between tree species and site. Model selection was based on AIC values, and the final model retained only significant predictors.

Fine and coarse root biomass were analysed using linear mixed-effects models. For each root type, a global model included soil depth, tree species, site, and the interaction between species and site as fixed effects, with tree identity included as a random effect to account for repeated sampling.

To examine the relationship between stem CH_4 emissions and belowground variables, we used Pearson's correlation coefficients. Correlations were performed separately for várzea and igapó forests, and then further stratified by species and stem height. Fine and coarse root biomass were analysed at depths of 50, 100, and 150 cm. A significance threshold of $P<0.05$ was used throughout, with *P*-values between 0.05 and 0.1 interpreted as indicative of trends. All reported correlations include Pearson's *r* and associated *P*-values.

Results

Stem CH_4 emission magnitude and variability across sites and species

Across both forest types and species, there was a pronounced vertical decline in emissions: stem CH_4 emissions were consistently higher at 30–60 cm than at 70–100 cm ($P<0.001$; Fig. 2). At a given height, emissions were also higher in várzea than in igapó forests ($P=0.041$; Fig. 2). Although mean emissions differed between tree species within sites, species identity did not explain significant variation in stem CH_4 emissions once site and height were accounted for – the final model for CH_4 emissions only retained site and height as fixed effects. Stem CH_4 emissions exhibited substantial variability among individual trees, particularly at 30–60 cm height, with the greatest variability observed in the várzea forest.

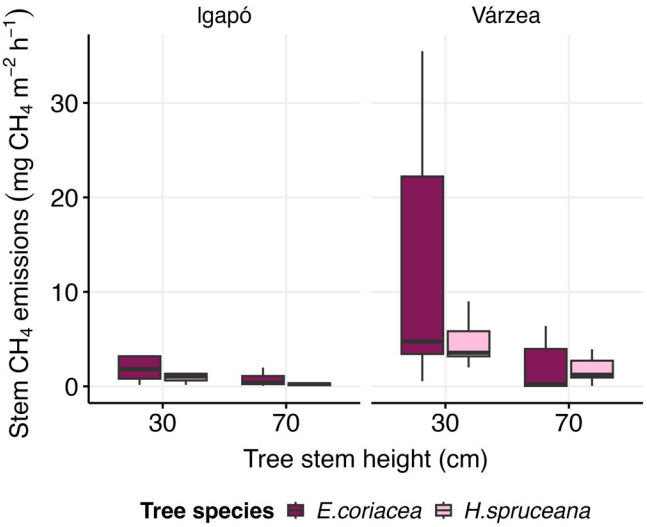

Fig. 2 Stem CH_4 emissions for two species (*Eschweilera coriacea*, $n=10$; *Hevea spruceana*, $n=10$) in two floodplain forest types (várzea, igapó), measured at two heights (30–60 cm and 70–100 cm relative to the water surface). Emissions (mg CH_4 m^{-2} h^{-1}) are reported per unit area of the stem surface enclosed by the chamber. The central line represents the median; the box spans the interquartile range (IQR; 25th–75th percentiles); and the whiskers extend to the most extreme values within 1.5 × IQR.

In the igapó forest, mean stem CH_4 emissions at 30–60 cm were lower overall, averaging 3.14 ± 3.86 mg CH_4 m^{-2} h^{-1} for *E. coriacea* and 0.92 ± 0.53 mg CH_4 m^{-2} h^{-1} for *H. spruceana*. At 70–100 cm, emissions further declined to 0.75 ± 0.79 mg CH_4 m^{-2} h^{-1} for *E. coriacea* and 0.24 ± 0.14 mg CH_4 m^{-2} h^{-1} for *H. spruceana*. At 30- to 60-cm stem height in the várzea forest, mean stem CH_4 emissions were 13.3 ± 15.0 mg CH_4 m^{-2} h^{-1} for *E. coriacea* and 4.71 ± 2.77 mg CH_4 m^{-2} h^{-1} for *H. spruceana*. At 70–100 cm, emissions declined substantially in both species, averaging 2.12 ± 2.91 mg CH_4 m^{-2} h^{-1} for *E. coriacea* and 1.77 ± 1.55 mg CH_4 m^{-2} h^{-1} for *H. spruceana*.

Porewater chemistry and CH_4 production potential variability across depth and sites

No significant interannual differences (2019 vs 2021) were found in porewater chemistry measured (DO, pH, and EC) after accounting for soil depth ($P > 0.05$; Table 2). Based on the absence of detectable year effects, we assumed that belowground parameters measured in 2021 were representative of belowground conditions during the 2022 stem CH_4 emission measurements (Table 2). Accordingly, tree stem CH_4 emissions were modelled against belowground parameters measured in 2021.

Dissolved CH_4 concentrations exhibited strong vertical structure across soil profiles, with concentrations highest at 0- to 50-cm soil depth and declining with depth (Table 2; Fig. 3). In the mixed-effects model, dissolved CH_4 decreased significantly with increasing soil depth, was higher beneath *H. spruceana* than *E. coriacea*, and increased with increasing MPP.

Across both sites, porewater chemistry and MPP displayed pronounced depth-related gradients. In igapó soils, dissolved CH_4 concentrations were lower overall but followed similar depth-related declines, peaking at 50 cm and averaging 64.6 µmol l^{-1}. MPP was lower than in várzea, averaging 1.14 mg CH_4 m^{-2} h^{-1} at 30 cm and declining to 0.29 mg CH_4 m^{-2} h^{-1} at 150 cm (Table 2). Igapó soils remained more acidic and less conductive than várzea soils, with pH ranging from 3.82 to 6.7 and EC averaging 38.8 µS cm^{-1} at 50 cm, declining further with depth. DO concentrations decreased from 4.56 mg l^{-1} at 50 cm to 1.11 mg l^{-1} at 150 cm, while DOC declined from 19.7 to 3.9 mg l^{-1} across the profile (Table 2).

In várzea soils, dissolved CH_4 averaged 129 µmol l^{-1} at 50 cm and declined to 23.2 µmol l^{-1} at 150 cm, while MPP was greatest in shallow soils (mean 9.27 mg CH_4 m^{-2} h^{-1} at 30 cm) and decreased sharply with depth. DO concentrations declined from 3.0 mg l^{-1} at 50 cm to 0.25 mg l^{-1} at 150 cm, and DOC concentrations decreased from 8.32 to 2.9 mg l^{-1} across the same depth interval. Soil water pH ranged from near-neutral values in surface soils to slightly lower values at depth, while EC remained comparatively high throughout the profile (Table 2).

Dissolved CH_4 differed significantly across tree species, with greater quantities found in depths associated with *H. spruceana*, compared with *E. coriacea* ($P < 0.01$) – a pattern repeated in both igapó and várzea. Despite clear site-level differences in porewater chemistry and MPP, site, pH, DO, EC, DOC, and the site × species interaction did not explain additional variation in dissolved CH_4 once soil depth, tree species, and MPP were included in the model ($P > 0.05$).

Root biomass distribution variability across depth and sites

Root biomass was strongly structured by soil depth, with both fine and coarse roots concentrated in the upper 0- to 50-cm soil layer (Table 2). Root biomass declined sharply with increasing depth and was negligible below 50 cm. No significant differences were found between the two tree species for either fine or coarse root biomass at any depth.

In the igapó forest, fine-root biomass at 0–50 cm averaged 945 ± 486 g m^{-3}, while coarse root biomass was 949 ± 606 g m^{-3}. Root biomass at greater depths was negligible: fine roots averaged 23.9 ± 31 g m^{-3} at 50–100 cm and 0.113 ± 0.621 g m^{-3} at 100–150 cm. Coarse root biomass at these depths was 4.38 ± 14.7 g m^{-3} and 1.93 ± 7.56 g m^{-3}, respectively (Table 2). The várzea forest exhibited a similar depth-related pattern, but with higher biomass values than igapó (Table 2). Fine root biomass at 0–50 cm averaged 1257 ± 700 g m^{-3}, while coarse root biomass averaged 978 ± 540 g m^{-3}. At 50–100 cm, fine and coarse root biomass declined to 5.07 ± 13.6 g m^{-3} and 1.99 ± 5.29 g m^{-3}, respectively, and decreased further at 100–150 cm to 2.61 ± 14.3 g m^{-3} for fine roots, with coarse roots at 7 ± 20.3 g m^{-3} (Table 2).

Relationships between belowground variables and stem CH_4 emissions

With lower overall stem CH_4 emissions in igapó, the relationship between belowground variables and emissions was weaker and not statistically significant (Table S2). Across all trees, moderate positive trends were observed for MPP ($r = 0.52$, $P = 0.067$) and EC ($r = 0.49$, $P = 0.081$), but these relationships were not significant. Fine-root biomass at 0–50 cm depth was weakly correlated with 30- to 60-cm stem emission ($r = 0.26$, $P = 0.36$), and no relationship was detected with coarse root biomass. Species-level analyses revealed no meaningful correlations for *E. coriacea* and for *H. spruceana*. At 70- to 100-cm stem height, emissions were lower, and all correlations with belowground variables diminished and were statistically nonsignificant (Table S3).

In várzea, stem CH_4 emissions at 30–60 cm height showed moderate-to-strong correlations with several belowground variables. Across all trees, pH ($r = 0.60$, $P = 0.026$) and EC ($r = 0.57$, $P = 0.034$) were the best predictors of stem emissions at 30–60 cm (Table S2). MPP in topsoil (0–50 cm) was also correlated positively with 30- to 60-cm emissions ($r = 0.62$, $P = 0.021$). Root biomass further explained variation in stem emissions. Fine-root biomass at 0–50 cm depth showed a positive correlation with stem emissions at 30–60 cm ($r = 0.49$; $P = 0.048$). Coarse root biomass was not significantly associated with stem emissions. Species-specific patterns revealed stronger belowground coupling in *E. coriacea*. For this species, 30- to 60-cm stem emission was significantly correlated with EC ($r = 0.70$, $P = 0.043$) and MPP ($r = 0.68$, $P = 0.048$), with a borderline association with fine-root biomass ($r = 0.56$, $P = 0.061$). For *H.*

Table 2 Belowground parameters measured at three soil depths (0–50 cm, 50–100 cm, and 100–150 cm) during the wet seasons of 2019 and 2021.

Study year	Study site	Tree species	Soil depth (cm)	EC ± SD ($\mu S\ cm^{-1}$)	pH ± SD	Dissolved CH_4 ± SD (μmol^{-1})	DO ± SD ($mg\ l^{-1}$)	DOC ± SD ($mg\ l^{-1}$)	MPP ± SD ($mg\ CH_4\ m^{-2}\ h^{-1}$)	Fine-root biomass ($g\ m^{-3}$)	Coarse root biomass ($g\ m^{-3}$)
2019	Igapó	*H. spruceana*	0–50	40.2 ± 6.4	4.9 ± 0.6	–	4.5 ± 1.1	–	–	817 ± 255	1029 ± 789
			50–100	26.7 ± 6.6	4.4 ± 0.8	–	3.1 ± 0.3	–	–	29.1 ± 34.4	8.75 ± 20.1
			100–150	17 ± 4.6	4.2 ± 0.7	–	1.3 ± 0.6	–	–	0.22 ± 0.87	1.46 ± 5.65
		E. coriacea	0–50	38.4 ± 3.97	5.29 ± 1.01	–	4.93 ± 1.08	–	–	1073 ± 622	867 ± 351
			50–100	24.9 ± 5.14	5.29 ± 1.07	–	2.78 ± 0.51	–	–	18.7 ± 29.3	0 ± 0
			100–150	12.6 ± 2.39	4.67 ± 1.42	–	1.08 ± 0.46	–	–	0 ± 0	2.39 ± 9.26
	Várzea	*H. spruceana*	0–50	128 ± 33.1	7.04 ± 0.44	–	3.17 ± 1.43	–	–	1394 ± 714	1098 ± 632
			50–100	72.7 ± 11.5	6.61 ± 0.98	–	1.47 ± 0.38	–	–	10.13 ± 18.2	2.24 ± 6.7
			100–150	54.5 ± 9.26	5.78 ± 1.34	–	0.37 ± 0.21	–	–	0 ± 0	4.33 ± 11.97
		E. coriacea	0–50	114 ± 26.6	6.55 ± 0.49	–	3.5 ± 0.77	–	–	1120 ± 682	857 ± 415
			50–100	77.5 ± 15.4	6.75 ± 0.44	–	1.6 ± 0.27	–	–	0 ± 0	1.74 ± 3.61
			100–150	57.2 ± 11.2	6.41 ± 0.22	–	0.39 ± 0.16	–	–	5.22 ± 20.3	9.67 ± 26.4
2021	Igapó	*H. spruceana*	0–50	39.5 ± 7.4	4.7 ± 0.7	69.6 ± 15.1	4.3 ± 1	19.8 ± 7.1	0.76 ± 0.11	–	–
			50–100	26.7 ± 7.5	4.5 ± 0.7	42.7 ± 5.4	2.9 ± 0.6	10.9 ± 3.6	0.44 ± 0.07	–	–
			100–150	16.3 ± 3.6	4.4 ± 0.8	12.8 ± 5.6	1.3 ± 0.6	4.0 ± 2.3	0.29 ± 0.05	–	–
		E. coriacea	0–50	38.3 ± 5.5	5.0 ± 1.1	59.6 ± 26.7	4.8 ± 0.9	19.6 ± 7.8	0.72 ± 0.12	–	–
			50–100	23.6 ± 4.2	4.8 ± 1.1	20.9 ± 10.4	2.7 ± 0.8	8.1 ± 1.0	0.47 ± 0.09	–	–
			100–150	11.9 ± 1.4	4.7 ± 1.3	7.9 ± 7.8	0.9 ± 0.3	3.8 ± 2.2	0.29 ± 0.02	–	–
	Várzea	*H. spruceana*	0–50	111 ± 19.7	6.5 ± 0.3	153 ± 37.3	2.7 ± 1.3	9.5 ± 1.3	5.07 ± 0.98	–	–
			50–100	75.4 ± 11.1	6.2 ± 0.7	76.0 ± 22.1	1.3 ± 0.5	4.7 ± 2.6	3.21 ± 0.65	–	–
			100–150	50.8 ± 9.4	5.7 ± 1.4	34.2 ± 8.3	0.2 ± 0.2	2.6 ± 0.6	1.44 ± 0.24	–	–
		E. coriacea	0–50	117 ± 31.7	6.83 ± 0.3	104.1 ± 41	3.3 ± 0.8	7.1 ± 2.1	5.42 ± 0.64	–	–
			50–100	76.6 ± 18.8	6.76 ± 0.3	35.8 ± 13.7	1.6 ± 0.5	5.7 ± 2.2	2.76 ± 0.37	–	–
			100–150	52.9 ± 14.3	6.6 ± 0.4	12.1 ± 12.6	0.3 ± 0.1	3.2 ± 1.3	1.20 ± 0.36	–	–

Samples are presented separately by site (igapó and várzea) and by the tree species associated with the piezometer locations. Results are expressed as mean ± SD.

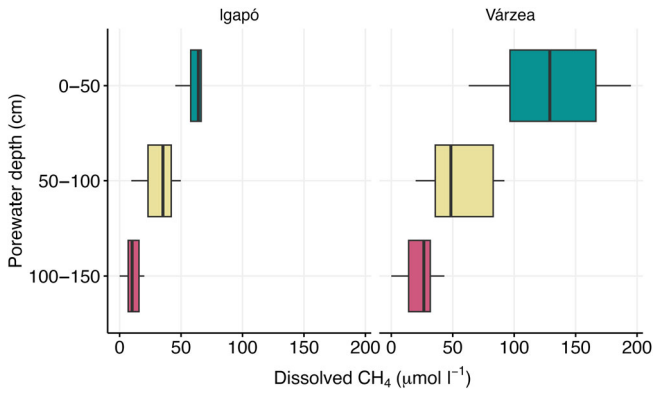

Fig. 3 Dissolved CH_4 concentrations (μmol L^{-1}) at three soil depths (0–50, 50–100, 100–150 cm) around each sampled tree across igapó and várzea forest plots. The central line represents the median; the box spans the interquartile range (IQR; 25^{th}–75^{th} percentiles); and the whiskers extend to the most extreme values within 1.5 × IQR.

spruceana, correlations were weaker and nonsignificant (e.g. MPP: $r = 0.41$, $P = 0.18$). As in igapó, correlations weakened at 70- to 100-cm stem height (Table S3).

Discussion

Our study demonstrates that stem CH_4 emissions in Amazonian floodplain forests are more strongly regulated by site characteristics (white-water vs black-water) than species identity (*E. coriacea* vs *H. spruceana*). In the high-emitting, white water site, we found that shallow soil biogeochemical properties were the best predictors of stem emissions at 30- to 60-cm stem height.

Site-level biogeochemistry as the dominant control

Stem CH_4 emissions were significantly higher in várzea than in igapó (*c.* 4× higher in várzea than igapó), irrespective of species or stem height (Fig. 2), consistent with basin-scale assessments that white-water floodplains emit more CH_4 than black-water systems (Pangala *et al.*, 2017; Gauci *et al.*, 2022). Várzea porewaters had higher EC, near-neutral pH, lower DO, and higher dissolved CH_4, conditions favourable for methanogenesis (Segers, 1998; Conrad, 2007; Bridgham *et al.*, 2013). By contrast, igapó porewaters were acidic and more oxygenated, conditions that constrain methanogenesis and favour CH_4 oxidation (Teh *et al.*, 2005; Laanbroek, 2010; Table 2). Independent observations from Amazon floodplain lakes similarly report higher CH_4 production and greater diffusive and ebullitive emissions in white-water settings than in black-water environments (Engle & Melack, 2000; Barbosa *et al.*, 2016, 2021). Given our measurements were made within a single flooded season, hydrology cannot explain the order-of-magnitude between-site differences in stem emissions; instead, the contrast in porewater biogeochemistry appears to be the more plausible explanation.

Across both forests, the 0- to 50-cm soil layer emerged as the primary zone of CH_4 supply, with MPP, dissolved CH_4, and fine-root biomass generally declining with depth (Table 2). This vertical pattern suggests that deeper layers (50–100 cm and 100–150 cm) contributed less to CH_4 production and availability than the shallow soil, consistent with previous wetland studies showing that root activity, fresh carbon inputs, and strong redox gradients concentrate CH_4 production near the surface (Segers, 1998; Aulakh *et al.*, 2001; Le Mer & Roger, 2001; Liu *et al.*, 2012; Määttä & Malhotra, 2024). However, this shallow active zone was more pronounced in várzea than in igapó, with higher MPP and dissolved CH_4 concentrations in the 0- to 50-cm layer, and only in várzea did these shallow belowground variables show clear relationships with stem CH_4 emissions (Tables S2 and S3). Together, these results suggest that although the same near-surface depth zone is important in both forests, it contributes more strongly to stem CH_4 emissions in várzea than in igapó.

In várzea, basal stem CH_4 emissions were closely linked to shallow methanogenic conditions, rather than to bulk carbon availability (Table S2). Near-surface porewater chemistry and MPP explained variation in basal stem emissions, while DOC showed no relationship, indicating that process controls were more important than substrate quantity alone. Associations with fine roots were confined to the upper soil layers, again pointing to a shallow source zone. By contrast, basal stem emissions in igapó showed little sensitivity to below-ground variables, likely because acidic and relatively oxygenated conditions constrained CH_4 production despite high DOC availability. A similar pattern, in which high DOC does not necessarily translate into high net CH_4 emissions, has been reported in Amazon black-water systems and tropical peat swap forests (Pangala *et al.*, 2013, 2017; Sawakuchi *et al.*, 2014; Girkin *et al.*, 2020; Somers *et al.*, 2023).

Our measurements of MPP and dissolved CH_4 integrate the net effect of several belowground processes that were not quantified directly but are known to influence CH_4 production and availability in wetlands. Variation in litter inputs and quality, carbon-to-nitrogen (C : N) ratios, nutrient status, and the availability of alternative electron acceptors such as nitrate, ferric iron, and sulphate can all stimulate or suppress CH_4 production by altering substrate supply and redox constraints, as well as by shifting competition among microbial communities (Le Mer & Roger, 2001; Conrad, 2007; Bridgham *et al.*, 2013). The strong correlation between basal stem emission (30–60 cm), MPP, and dissolved CH_4 in the 0- to 50-cm layer in várzea indicates that these unmeasured processes likely acted through their effects on shallow CH_4 production, but explicitly quantifying litter inputs/-quality, C : N ratio, nutrient, and redox chemistry may help explain residual within-site variability.

Species identity as a secondary driver

Tree species identity exerted only a secondary influence on stem CH_4 emissions relative to site-level biogeochemistry. Although mean stem emissions differed between *E. coriacea* and *H. spruceana* within sites, species were not retained as a significant predictor once site and stem height were included in the model.

This indicates that species identity, and by implication wood density alone, cannot explain the major spatial differences in stem CH_4 emissions observed between white-water várzea and black-water igapó forests.

This is particularly notable because our species comparison was designed around contrasting wood density. Based on previous work, lower wood density is often expected to promote higher stem CH_4 emissions by reducing resistance to internal gas transport (Covey *et al.*, 2012; Pangala *et al.*, 2013; van Haren *et al.*, 2021; Soosaar *et al.*, 2022). However, the opposite pattern was observed here: *E. coriacea* (high density, 0.6–0.9 g cm^{-3}; Table S1) consistently emitted more CH_4 than *H. spruceana* (low density, 0.23–0.7 g cm^{-3}; Table S1), especially in várzea. Emissions ranged from 0.007 to 35.5 mg CH_4 m^{-2} h^{-1} in *E. coriacea*, nearly fourfold higher at maximum than *H. spruceana* (0.04–9.15 mg CH_4 m^{-2} h^{-1}). However, this comparison should be interpreted cautiously, as our inference is based on only two co-occurring species and uses species identity as a proxy for contrasting wood density rather than directly testing the broader range of woody traits across multiple floodplain taxa.

While wood traits are shown to influence gas transport and in stem CH_4 production and uptake (Soosaar *et al.*, 2022; Epron *et al.*, 2023), they cannot account for the order-of-magnitude differences observed between várzea and igapó for the same species. Our results are therefore more consistent with a framework in which species traits modulate emissions once CH_4 is available, rather than acting as the dominant control over spatial patterns in stem CH_4 emissions (Warner *et al.*, 2017; Pitz *et al.*, 2018; Barba *et al.*, 2019; Covey & Megonigal, 2019). Other stem and bark traits, including porosity, permeability, moisture content, parenchyma fraction, lenticel abundance, internal stem chemistry, bark and stem methanotrophy, and the abundance or activity of methanogenic and methanotrophic communities within bark and wood tissues, likely govern gas transport and in-stem CH_4 cycling, and may all therefore contribute to variation in net stem emissions (Covey & Megonigal, 2019; Yip *et al.*, 2019; Jeffrey *et al.*, 2021; Mochidome & Epron, 2024).

Intra- and interspecific variability

Pairing each tree stem emission with the belowground profile allowed us to examine variability within sites and between co-occurring species. Despite the dominant role of site-level biogeochemistry, stem CH_4 emissions varied by an order of magnitude among colocated trees in várzea, whereas ranges in igapó were much narrower (Fig. 2). This within-site variability has been reported in other wetland forests (Pangala *et al.*, 2013; Cugler *et al.*, 2024) and in global syntheses (Barba *et al.*, 2019), but our results suggest it is site-contingent: variability was greater in nutrient-rich, near-neutral várzea and dampened in acidic, more oxygenated igapó, consistent with geochemical constraints on CH_4 production and oxidation (Yip *et al.*, 2019; Li *et al.*, 2020; Wang *et al.*, 2021). Thus, when porewater chemistry is conducive to CH_4 production, both mean stem emissions and tree-to-tree variability appear to increase, but the cause of increased variability is unknown.

Stem CH_4 emissions declined significantly with stem height (30–60 cm > 70–100 cm; Fig. 2). Similar decreases in emissions with stem height are widely reported across tropical, temperate, and boreal forests and are consistent with predominantly diffusive transport from a soil source, with strongest gradients at the stem base (Rusch & Rennenberg, 1998; Pangala *et al.*, 2017; Pitz & Megonigal, 2017; Sjögersten *et al.*, 2020; Jeffrey *et al.*, 2021; Gauci *et al.*, 2022; Machacova *et al.*, 2023). However, the magnitude of this decline differed between species: emissions declined *c.* sixfold with height in *E. coriacea* but *c.* two- to threefold in *H. spruceana* across sites. This suggests that species-specific traits may regulate gas conductance, transport, and degassing along the stem (Covey & Megonigal, 2019; Mochidome & Epron, 2024). Potential in-stem CH_4 cycling (production and oxidation) may further reshape these vertical emission patterns (Yip *et al.*, 2019; Li *et al.*, 2020; Zhou *et al.*, 2021; Epron *et al.*, 2023). Our observations of wet, degraded heartwood in *E. coriacea* are consistent with this possibility, though confirmation would require further investigation. The measured belowground variables explained only part of the within-site and between-species variation in stem CH_4 emissions. It appears that once CH_4 is available in the near-surface, additional stem-level traits likely shape stem emissions.

Root–soil interactions and CH_4 supply

Across both forest types, the upper 0- to 50-cm soil layer showed consistently elevated MPP, dissolved CH_4, and fine-root biomass relative to deeper soils (50–100 and 100–150 cm; Table 2). This pattern indicates a shallow active zone for potential CH_4 supply (increased CH_4 production and availability), consistent with previous wetland studies, showing that fresh carbon inputs, strong redox gradients, and root activity tend to concentrate CH_4 production in near-surface soils (Segers, 1998; Silver *et al.*, 1999; Conrad, 2007). Within várzea, basal (30–60 cm) stem CH_4 emission was positively correlated with fine-root biomass between 0 and 50 cm, whereas coarse roots showed no relationship. This suggests that fine roots may be more important than coarse roots in shaping the shallow belowground environment linked to stem CH_4 emissions. Through their greater surface area and metabolic activity, fine roots can influence rhizosphere carbon inputs, oxygen availability, and water uptake, thereby affecting CH_4 production, availability, and transport to the stem (Aulakh *et al.*, 2001; Bridgham *et al.*, 2013).

In várzea, the two species exhibited distinct associations with below-ground variables measured (Table S3): for *E. coriacea*, basal emissions were strongly correlated with EC and MPP and showed a near-significant correlation with fine-root biomass; for *H. spruceana*, pH and EC were the dominant controls. In igapó, correlations between stem emissions and belowground variables were weak or absent, consistent with acidic, more oxygenated porewaters limiting methanogenesis and reducing variation in CH_4 supply.

Our data collectively suggest a supply-then-transport hypothesis: where shallow porewater chemistry favours methanogenesis (várzea), dense fine roots likely enhance CH_4 supply to stems, increasing mean emissions and tree-to-tree variance; where

chemistry constrains methanogenesis (igapó), this root–stem coupling weakens, and emissions remain low. In this framework, species and wood traits act downstream of supply, modulating transport and in-stem processing once CH_4 is available, rather than determining supply itself (Pangala *et al.*, 2015; Covey & Megonigal, 2019; van Haren *et al.*, 2021; Soosaar *et al.*, 2022; Moisan *et al.*, 2024).

Conclusions

Our findings demonstrate that stem CH_4 emissions in Amazon floodplain forests are controlled primarily by site-level subsurface biogeochemistry rather than by species identity alone. Across two co-occurring tree species with contrasting wood density, emissions were consistently higher in white-water várzea than in black-water igapó. By linking stem emissions to porewater chemistry, MPP, and fine-root biomass, this study provides mechanistic insight into why white-water várzea forests function as CH_4 hotspots, while black-water igapó forests act as weaker sources. Together, these results indicate that variation in shallow methanogenic conditions or a near-surface zone of CH_4 supply between floodplain types underpins spatial variation in Amazonian tree stem CH_4 emissions. Species traits may still influence stem CH_4 emissions, but they appear to act as secondary modifiers rather than primary controls and should be examined more directly in future studies. More broadly, our results indicate that basin-scale assessments of Amazon floodplain CH_4 emissions will need to incorporate biogeochemical gradients and root-zone properties to better represent spatial variation in tree stem emissions. Scaling based solely on tree species composition will misrepresent emission patterns.

Acknowledgements

This research was funded by a Royal Society Research Grant (RGF\R1\180042) awarded to SRP. HB was supported by a studentship associated with this grant. SRP acknowledges support from the Royal Society Dorothy Hodgkin research fellowship (DH160111) and Royal Society enhancement award (RGF\EA \180042). AMH acknowledges support from the Stanford Woods Institute for the Environment, the Gordon and Betty Moore Foundation, Grant GBMF11519 (Advancing the understanding of methane emissions from tropical wetlands), and the Steven and Roberta Denning International Research Fund. The authors would like to thank the Mamirauá Institute for Sustainable Development for support throughout the study. We thank M. Castro, J. Castro, A. Silva, J. Carvalho, and E. Martins for all their fieldwork support and guidance.

Competing interests

None declared.

Author contributions

SRP and HRB conceived the study. HRB was supervised by SRP, NPM and AMH. HRB coordinated logistics and led fieldwork with support from CG, JL and RNdS. RNdS and SRP collected the 2019 and 2021 belowground datasets; SRP and RNdS also established plots and installed instrumentation. DMOE supervised and trained HRB in laboratory analyses of belowground properties and supported subsequent data interpretation. DG and LPR facilitated site access and permissions. HRB and SRP analysed the data, and HRB, SRP and NPM wrote the manuscript; all authors contributed to revisions and approved the final version.

ORCID

Holly R. Blincow https://orcid.org/0009-0009-1866-1089
Dafydd M. O. Elias https://orcid.org/0000-0002-2674-9285
Carla Gomez https://orcid.org/0000-0002-2972-2731
Darlene Gris https://orcid.org/0000-0003-1165-9997
Alison M. Hoyt https://orcid.org/0000-0003-0813-5084
Jack Lamb https://orcid.org/0000-0002-6584-7697
Niall P. McNamara https://orcid.org/0000-0002-5143-5819
Sunitha Rao Pangala https://orcid.org/0000-0002-0650-7721
Leonardo Pequeno Reis https://orcid.org/0000-0002-5829-1598

Data availability

Data available in article Supporting Information (Dataset S1).

References

Aulakh MS, Wassmann R, Bueno C, Rennenberg H. 2001. Impact of root exudates of different cultivars and plant development stages of rice (*Oryza sativa* L.) on methane production in a paddy soil. *Plant and Soil* **230**: 77–86.

Barba J, Bradford MA, Brewer PE, Bruhn D, Covey K, van Haren J, Megonigal JP, Mikkelsen TN, Pangala SR, Pihlatie M *et al.* 2019. Viewpoints Methane emissions from tree stems: a new frontier in the global carbon cycle. *New Phytologist* **222**: 18–28.

Barbosa PM, Melack JM, Amaral JHF, Linkhorst A, Forsberg BR. 2021. Large seasonal and habitat differences in methane ebullition on the Amazon floodplain. *Journal of Geophysical Research: Biogeosciences* **126**: e2020JG005911.

Barbosa PM, Melack JM, Farjalla VF, Amaral JHF, Scofield V, Forsberg BR. 2016. Diffusive methane fluxes from Negro, Solimões and Madeira rivers and fringing lakes in the Amazon basin. *Limnology and Oceanography* **61**(S1): S221–S237.

Bridgham SD, Cadillo-Quiroz H, Keller JK, Zhuang Q. 2013. Methane emissions from wetlands: biogeochemical, microbial, and modeling perspectives from local to global scales. *Global Change Biology* **19**: 1325–1346.

Cawley K, Goodman K, Weintraub S, Parker S. 2020. Neon user guide to dissolved gases in surface water. In NEONDISSGAS package.

Chave J, Coomes D, Jansen S, Lewis SL, Swenson NG, Zanne AE. 2009. Towards a worldwide wood economics spectrum. *Ecology Letters* **12**: 351–366.

Conrad R. 2007. Microbial ecology of methanogens and methanotrophs. *Advances in Agronomy* **96**: 1–63.

Cook S, Peacock M, Evans CD, Page SE, Whelan M, Gauci V, Khoon KL. 2016. Cold storage as a method for the long-term preservation of tropical dissolved organic carbon (DOC). *Mires and Peat* **18**: 1–8.

Covey KR, Megonigal JP. 2019. Methane production and emissions in trees and forests. *New Phytologist* **222**: 35–51.

Covey KR, Wood SA, Warren RJ, Lee X, Bradford MA. 2012. Elevated methane concentrations in trees of an upland forest. *Geophysical Research Letters* **39**: 15705.

Cugler G, Figueiredo V, Gauci V, Stauffer T, Peixoto RB, Rao Pangala S, Enrich-Prast A. 2024. Analysis of CH_4 and N_2O fluxes in the dry season: influence of soils and vegetation types in the pantanal. *Forests* **15**: 2224.

Engle D, Melack JM. 2000. Methane emissions from an Amazon floodplain lake: enhanced release during episodic mixing and during falling water. *Biogeochemistry* **51**: 71–90.

Epron D, Mochidome T, Tanabe T, Dannoura M, Sakabe A. 2023. Variability in stem methane emissions and wood methane production of different tree species in a cold temperate mountain forest. *Ecosystems* **26**: 784–799.

Furch K. 1997. Chemistry of varzea and igapo soils and nutrient inventory of their floodplain forests. In: *The central Amazon floodplain: ecology of a pulsing system*. Berlin Heidelberg, Germany: Springer, 47–67.

Furch K, Wolfgang J. 1997. Physicochemical conditions in the floodplains. In: *The central Amazon floodplain: ecology of a pulsing system*. Berlin Heidelberg, Germany: Springer, 69–108.

Gauci V, Figueiredo V, Gedney N, Pangala SR, Stauffer T, Weedon GP, Enrich-Prast A. 2022. Non-flooded riparian Amazon trees are a regionally significant methane source. *Philosophical Transactions of the Royal Society A: Mathematical, Physical and Engineering Sciences* **380**: 20200446.

Ge M, Korrensalo A, Laiho R, Kohl L, Lohila A, Pihlatie M, Li X, Laine AM, Anttila J, Putkinen A *et al.* 2024. Plant-mediated CH_4 exchange in wetlands: a review of mechanisms and measurement methods with implications for modelling. *Science of the Total Environment* **914**: 169662.

Girkin NT, Vane CH, Turner BL, Ostle NJ, Sjögersten S. 2020. Root oxygen mitigates methane fluxes in tropical peatlands. *Environmental Research Letters* **15**: 064013.

van Haren J, Brewer PE, Kurtzberg L, Wehr RN, Springer VL, Espinoza RT, Ruiz JS, Cadillo-Quiroz H. 2021. A versatile gas flux chamber reveals high tree stem CH_4 emissions in Amazonian peatland. *Agricultural and Forest Meteorology* **307**: 108504.

Hess LL, Melack JM, Affonso AG, Barbosa C, Gastil-Buhl M, Novo EMLM. 2015. Wetlands of the lowland Amazon basin: extent, vegetative cover, and dual-season inundated area as mapped with JERS-1 synthetic aperture radar. *Wetlands* **35**: 745–756.

Heuertz M, Caron H, Scotti-Saintagne C, Pétronelli P, Engel J, Tysklind N, Miloudi S, Gaiotto FA, Chave J, Molino J-F *et al.* 2020. The hyperdominant tropical tree *Eschweilera coriacea* (Lecythidaceae) shows higher genetic heterogeneity than sympatric *Eschweilera* species in French Guiana. *Plant Ecology and Evolution* **153**: 67–81.

Jeffrey LC, Maher DT, Chiri E, Leung PM, Nauer PA, Arndt SK, Tait DR, Greening C, Johnston SG. 2021. Bark-dwelling methanotrophic bacteria decrease methane emissions from trees. *Nature Communications* **12**: 1–8.

Jeffrey LC, Maher DT, Tait DR, Reading MJ, Chiri E, Greening C, Johnston SG. 2021. Isotopic evidence for axial tree stem methane oxidation within subtropical lowland forests. *New Phytologist* **230**: 2200–2212.

Jeffrey LC, Moras CA, Tait DR, Johnston SG, Call M, Sippo JZ, Jeffrey NC, Laicher-Edwards D, Maher DT. 2023. Large methane emissions from tree stems complicate the wetland methane budget. *Journal of Geophysical Research: Biogeosciences* **128**: e2023JG007679.

Junk WJ, Piedade MTF, Schöngart J, Cohn-Haft M, Adeney JM, Wittmann F. 2011. A classification of major naturally-occurring Amazonian lowland wetlands. *Wetlands* **31**: 623–640.

Laanbroek HJ. 2010. Methane emission from natural wetlands: interplay between emergent macrophytes and soil microbial processes. A mini-review. *Annals of Botany* **105**: 141–153.

Le Mer J, Roger P. 2001. Production, oxidation, emission and consumption of methane by soils: a review. *Production, Oxidation, Emission and Consumption of Methane by Soils: A Review* **37**: 25–50.

Li HL, Zhang XM, Deng FD, Han XG, Xiao CW, Han SJ, Wang ZP. 2020. Microbial methane production is affected by secondary metabolites in the heartwood of living trees in upland forests. *Trees-Structure and Function* **34**: 243–254.

Liu D, Ding W, Jia Z, Cai Z. 2012. The impact of dissolved organic carbon on the spatial variability of methanogenic archaea communities in natural wetland ecosystems across China. *Applied Microbiology and Biotechnology* **96**: 253–263.

Määttä T, Malhotra A. 2024. The hidden roots of wetland methane emissions. *Global Change Biology* **30**: e17127.

Machacova K, Warlo H, Svobodová K, Agyei T, Uchytilová T, Horáček P, Lang F. 2023. Methane emission from stems of European beech (*Fagus sylvatica*) offsets as much as half of methane oxidation in soil. *New Phytologist* **238**: 584–597.

Mochidome T, Epron D. 2024. Drivers of intra-individual spatial variability in methane emissions from tree trunks in upland forest. *Trees* **38**: 625–636.

Moisan MA, Lajoie G, Constant P, Martineau C, Maire V. 2024. How tree traits modulate tree methane fluxes: a review. *Science of the Total Environment* **940**: 173730.

Pangala SR, Enrich-Prast A, Basso LS, Peixoto RB, Bastviken D, Hornibrook ERC, Gatti LV, Marotta H, Calazans LSB, Sakuragui CM *et al.* 2017. Large emissions from floodplain trees close the Amazon methane budget. *Nature* **552**: 230–234.

Pangala SR, Gowing DJ, Hornibrook ERC, Gauci V. 2014. Controls on methane emissions from *Alnus glutinosa* saplings. *New Phytologist* **201**: 887–896.

Pangala SR, Hornibrook ERC, Gowing DJ, Gauci V. 2015. The contribution of trees to ecosystem methane emissions in a temperate forested wetland. *Global Change Biology* **21**: 2642–2654.

Pangala SR, Moore S, Hornibrook ERC, Gauci V. 2013. Trees are major conduits for methane egress from tropical forested wetlands. *New Phytologist* **197**: 524–531.

Parolin P, De Simone O, Haase K, Waldhoff D, Rottenberger S, Kuhn U, Kesselmeier J, Kleiss B, Schmidt W, Pledade MTF *et al.* 2004. Central Amazonian floodplain forests: tree adaptations in a pulsing system. *The Botanical Review* **70**: 357–380.

Pitz S, Megonigal JP. 2017. Rapid reports temperate forest methane sink diminished by tree emissions. *New Phytologist* **214**: 1432–1439.

Pitz S, Megonigal JP, Chang C-H, Szlávecz K. 2018. Methane fluxes from tree stems and soils along a habitat gradient. *Biogeochemistry* **137**: 307–320.

Poorter L, McDonald I, Alarcón A, Fichtler E, Licona J, Peña-Claros M, Sterck F, Villegas Z, Sass-Klaassen U. 2010. The importance of wood traits and hydraulic conductance for the performance and life history strategies of 42 rainforest tree species. *New Phytologist* **185**: 481–492.

Rusch H, Rennenberg H. 1998. Black alder (*Alnus glutinosa* (L.) Gaertn.) trees mediate methane and nitrous oxide emission from the soil to the atmosphere. *Plant and Soil* **201**: 1–7.

Saunois M, Martinez A, Poulter B, Zhang Z, Raymond PA, Regnier P, Canadell JG, Jackson RB, Patra PK, Bousquet P *et al.* 2025. Global Methane Budget 2000–2020. *Earth System Science Data* **17**: 1873–1958.

Sawakuchi HO, Bastviken D, Sawakuchi AO, Krusche AV, Ballester MVR, Richey JE. 2014. Methane emissions from Amazonian Rivers and their contribution to the global methane budget. *Global Change Biology* **20**: 2829–2840.

Segers R. 1998. Methane production and methane consumption: a review of processes underlying wetland methane fluxes. *Biogeochemistry* **41**: 23–51.

Silver WL, Lugo AE, Keller M. 1999. Soil oxygen availability and biogeochemistry along rainfall and topographic gradients in upland wet tropical forest soils. *Biogeochemistry* **44**: 301–328.

Sjögersten S, Siegenthaler A, Lopez OR, Aplin P, Turner B, Gauci V. 2020. Methane emissions from tree stems in neotropical peatlands. *New Phytologist* **225**: 769–781.

Somers LD, Hoyt A, Cobb AR, Isnin S, Suhip MAABH, Sukri RS, Gandois L, Harvey C. 2023. Processes controlling methane emissions from a tropical peatland drainage canal. *Journal of Geophysical Research: Biogeosciences* **128**: e2022JG007194.

Soosaar K, Schindler T, Machacova K, Pärn J, Fachín-Malaverri LM, Rengifo-Marin JE, Alegría-Muñoz W, Jibaja-Aspajo JL, Negron-Juarez R, Zárate-Gómez R *et al.* 2022. High methane emission from palm stems and nitrous oxide emission from the soil in a Peruvian Amazon peat swamp forest. *Frontiers in Forests and Global Change* **5**: 849186.

Steege HT, Pitman NCA, Sabatier D, Baraloto C, Salomão RP, Guevara JE, Phillips OL, Castilho CV, Magnusson WE, Molino JF *et al.* 2013. Hyperdominance in the Amazonian tree flora. *Science* **342**: 1243092.

Teh YA, Silver WL, Conrad ME. 2005. Oxygen effects on methane production and oxidation in humid tropical forest soils. *Global Change Biology* **11**: 1283–1297.

Wang ZP, Li HL, Wu HH, Han SJ, Huang JH, Zhang XM, Han XG. 2021. Methane concentration in the heartwood of living trees and estimated methane emission on stems in upland forests. *Ecosystems* **24**: 1485–1499.

Wang ZP, Zeng D, Patrick WH. 1996. Methane emissions from natural wetlands. *Environmental Monitoring and Assessment* **42**: 143–161.

Warner DL, Villarreal S, McWilliams K, Inamdar S, Vargas R. 2017. Carbon dioxide and methane fluxes from tree stems, coarse woody debris, and soils in an upland temperate forest **20**: 1205–1216.

Wittmann F, Schöngart J, Junk WJ. 2010. Phytogeography, species diversity, community structure and dynamics of central Amazonian floodplain forests. In: Junk WJ, Piedade MTF, Wittmann F, Schöngart J, Parolin P, eds. *Amazonian floodplain forests, vol. 210*. Dordrecht, the Netherlands: Springer, 61–102. doi: 10.1007/978-90-481-8725-6_4.

Wittmann F, Schöngart J, Montero JC, Motzer T, Junk WJ, Piedade MTF, Queiroz HL, Worbes M. 2006. Tree species composition and diversity gradients in white-water forests across the Amazon basin. *Journal of Biogeography* **33**: 1334–1347.

Wycherley PR. 1992. The genus *Hevea* – botanical aspects. In: *Developments in crop science, vol 23*. Amsterdam, the Netherlands: Elsevier, 50–66. doi: 10.1016/B978-0-444-88329-2.50009-X.

Yang H, Wang S, Son R, Lee H, Benson V, Zhang W, Zhang Y, Zhang Y, Kattge J, Boenisch G *et al.* 2024. Global patterns of tree wood density. *Global Change Biology* **30**: e17224.

Yip DZ, Veach AM, Yang ZK, Cregger MA, Schadt CW. 2019. Methanogenic Archaea dominate mature heartwood habitats of Eastern Cottonwood (*Populus deltoides*). *New Phytologist* **222**: 115–121.

Zhou X, Zhang M, Krause SMB, Bu X, Gu X, Guo Z, Jia Z, Zhou X, Wang X, Chen X *et al.* 2021. Soil aeration rather than methanotrophic community drives methane uptake under drought in a subtropical forest. *Science of the Total Environment* **792**: 148292.

Supporting Information

Additional Supporting Information may be found online in the Supporting Information section at the end of the article.

Dataset S1 Dataset of the present study.

Fig. S1 Photographs of plots, flooded forest, and stem chamber.

Table S1 Tree-level stem CH_4 emissions, wood density, and diameter at breast height (DBH) by plot.

Table S2 Pearson correlation coefficients (r) and corresponding P-values (P) for stem CH_4 emission and belowground variables.

Table S3 Pearson correlation coefficients (r) and associated P-values (P) for stem CH_4 emission and belowground variables, separated by tree species.

Please note: Wiley is not responsible for the content or functionality of any Supporting Information supplied by the authors. Any queries (other than missing material) should be directed to the *New Phytologist* Central Office.